

receiver sensitivity is attributed to variations in residual dispersion and OSNR at different wavelengths.

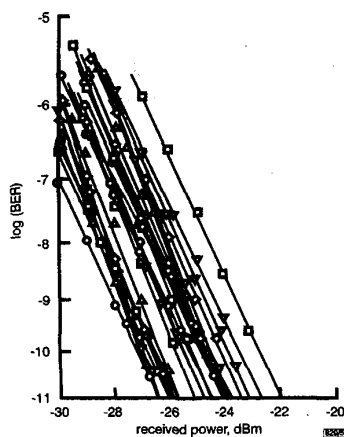


Fig. 5 BER measurements
2²³-1 NRZ PRBS

While several terabit/s capacity WDM transmission schemes have been demonstrated successfully, one issue still remains: how efficiently is the optical bandwidth utilised? This can be explained by the spectral efficiency defined as the aggregate transmission capacity (bit/s) divided by the optical bandwidth (Hz) used. In this experiment, a spectral efficiency of 0.32 bit/s/Hz was achieved, compared to a theoretical limit of 0.5 bit/s/Hz in NRZ format transmission.

In summary, we have described a 1 Tbit/s (40 Gbit/s × 25 ch) transmission experiment over 342 km of nonzero dispersion (True-Wave) fibre with a spectral efficiency of 0.32 bit/s/Hz. A 40 Gbit/s OTDM transmitter, 3R receiver, and gain-flattened, conventional EDFAs were employed. Fibre chromatic dispersion was effectively compensated for using negative-slope DCF.

Acknowledgment: We are grateful to Z.Y. Gills and R.B. Kummer for technical help. We also thank A.M. Glass and W.F. Brinkman for constant encouragement and support.

© IEE 1999

8 March 1999

Electronics Letters Online No: 19990444
DOI: 10.1049/el:19990444

C.D. Chen, I. Kim, O. Mizuhara, T.V. Nguyen, K. Ogawa, R.E. Tench, L.D. Tzeng and P.D. Yeates (Bell Laboratories, Lucent Technologies, Photonic Systems Technology Research Dept., 9999 Hamilton Blvd., Breinigsville, PA 18031, USA)

E-mail: ik@lucent.com

Note: Names listed in alphabetical order

References

- ONAKA, H., MIYATA, H., ISHIKAWA, G., OTSUKA, K., OOI, H., KAI, Y., KINOSHITA, S., SEINO, M., NISHIMOTO, H., and CHIKMA, T.: '1.1 Tbit/s WDM transmission over a 150 km 1.3 μm zero-dispersion single-mode fiber'. Optical Fiber Communication Conf., (OFC'96), San Jose, CA, February 1996, Postdeadline Paper PD19
- GNAUCK, A.H., CHRAPLYVY, A.R., TKACH, R.W., ZYSKIND, J.L., SULHOFF, J.W., LUCERO, A.J., SUN, Y., JOPSON, R.M., FORGHIERI, F., DEROSIER, R.M., WOLF, C., and MCCORMICK, A.R.: 'One terabit/s transmission experiment'. Optical Fiber Communication Conf., (OFC'96), San Jose, CA, February 1996, Postdeadline Paper PD20
- YANO, Y., ONO, T., FUKUCHI, K., ITO, T., YAMAZAKI, H., YAMAGUCHI, M., and EMURA, K.: '2.6 terabit/s WDM transmission experiment using optical duobinary coding'. European Conf. Optical Communication (ECOC'96), Oslo, September 1996, Paper ThB. 3.1
- SRIVASTAVA, A.K., SUN, Y., SULHOFF, J.W., WOLF, C., ZIRNGIBL, M., MONNARD, R., CHRAPLYVY, A.R., ABRAMOV, A.A., ESPINDOLA, R.P., STRASSER, T.A., PEDRAZZANI, J.R., VENGSARKAR, A.M., ZYSKIND, J.L., ZHOU, J., FERRAND, D.A., WYSOCKI, P.F., JUDKINS, J.B., and LI, Y.P.: '1 Tbit/s transmission of 100 WDM 10 Gb/s channels over 400 km of TrueWave fibre'. Optical Fiber Communication Conf. (OFC'98), San Jose, CA, February 1998, Postdeadline Paper PD10

- AISAWA, S., SAKAMOTO, T., FUKUI, M., KANI, J., JINNO, M., and OGUCHI, K.: 'Ultra-wide band, long distance WDM transmission demonstration: 1 Tbit/s (50 × 20 Gb/s), 600 km transmission using 1550 and 1580 nm wavelength bands'. Optical Fiber Communication Conf. (OFC'98), San Jose, CA, February 1998, Postdeadline Paper PD11
- CHEN, C.D., KIM, I., MIZUHARA, O., NGUYEN, T.V., OGAWA, K., TENCH, R.E., TZENG, L.D., and YEATES, P.D.: '1.2 Tbit/s WDM transmission experiment over 85 km fibre using 40 Gb/s line rate transmitter and 3R receiver'. Optical Fiber Communication Conf. (OFC'98), San Jose, CA, February 1998, Postdeadline Paper PD21
- CHEN, C.D., KIM, I., MIZUHARA, O., NGUYEN, T.V., OGAWA, K., TENCH, R.E., TZENG, L.D., and YEATES, P.D.: '40 Gbit/s × 35 ch (1.4 Tbit/s aggregate capacity) WDM transmission over 85 km standard singlemode fibre', *Electron. Lett.*, 1998, **34**, pp. 2370-2371
- MIYAMOTO, Y., YONENAGA, K., HIRANO, A., SHIMIZU, N., YONEYAMA, M., TAKARA, H., NOGUCHI, K., and TSUZUKI, K.: '1.04 Tbit/s DWDM transmission experiment based on alternate-polarisation 80-Gbit/s OTDM signals'. European Conf. Optical Communication (ECOC'98), Madrid, Spain, September 1998, Postdeadline Paper

Dual resonant peaks of LP₀₁₅ cladding mode in long-period gratings

Xuewen Shu, Xuemei Zhu, Qinglin Wang, Shan Jiang, Wei Shi, Zhijian Huang and Dexiu Huang

It is found that the coupling of the guided core mode to a higher order cladding mode may lead to dual resonant wavelengths in long-period gratings (LPGs). The dual peaks of the LP₀₁₅ cladding mode have been observed to shift towards each other during the second exposure of a 100 μm period grating. It is also shown that the resonant wavelengths of LPGs can be tuned over a wide range by the post-exposure technique.

Introduction: Long-period gratings (LPGs) are very attractive for both telecommunications and sensing applications owing to their ease of fabrication, low insertion losses, low levels of back-reflection and compact sizes. Various devices based on LPGs have been demonstrated, such as band rejection filters [1], EDFA gain equalisers [2], notch filters [3], mode converters [4] and fibre sensors [5]. An LPG couples light from the guided fundamental mode into the forward propagating cladding modes when the phase matching conditions are satisfied. To benefit both fabrication and applications, it is necessary to determine the characteristics of the resonant peaks, which have recently been studied both theoretically and experimentally [1, 6-8]. Most work to date has focused on the resonant peaks of lower order cladding modes, which are shown to move to longer wavelengths in the growth process [1]. Recent research has shown that the resonant peaks of higher order cladding modes may shift to shorter wavelengths as the grating becomes stronger [8]. Despite impressive results, the characteristics of the resonant peaks have not yet been fully investigated. In this Letter, we report, for the first time to our knowledge, that coupling between the guided fundamental mode and a higher order cladding mode may lead to two resonant wavelengths and that the two peaks of the LP₀₁₅ mode in a 100 μm period grating were observed to move closer and closer until they almost disappeared during the second exposure of the grating. It is also found that the resonant wavelengths of an LPG can be tuned over a wide range by means of the post-exposure technique.

Experiment: First, a 25 mm long LPG with a period of 100 μm was written in a hydrogen-loaded Corning singlemode fibre using a KrF excimer laser (248 nm) through an amplitude mask, and followed by an annealing process at 200 °C for 7 h. The transmission spectrum of the annealed grating (termed 'initial') is shown in Fig. 1a. Two weak resonant peaks separated by ~300 nm are observed in the wavelength range 1100-1500 nm.

We then exposed the grating to the excimer laser again without using the amplitude mask. The energy of the laser radiation was ~260 mJ/pulse with a repetition rate of 10 Hz. The transmission spectra of the grating were monitored by an optical spectrum analyser. The transmission spectra taken at various pulse shots are

shown in Fig. 1*b-e*. Comparing Fig. 1*b* with Fig. 1*a*, it is found that the two resonant peaks shift towards each other and their depths both increased although no amplitude mask was used. As the shots continued, the two peaks moved closer and closer together until they coincided with each other, as shown in Fig. 1*d*. When there was only one resonant peak left, further shots weakened the resonant coupling. As shown in Fig. 1*e*, the resonant peak almost disappeared after 25000 shots. However, both resonant peaks reappeared after the grating was annealed again, as shown in Fig. 1*f*.

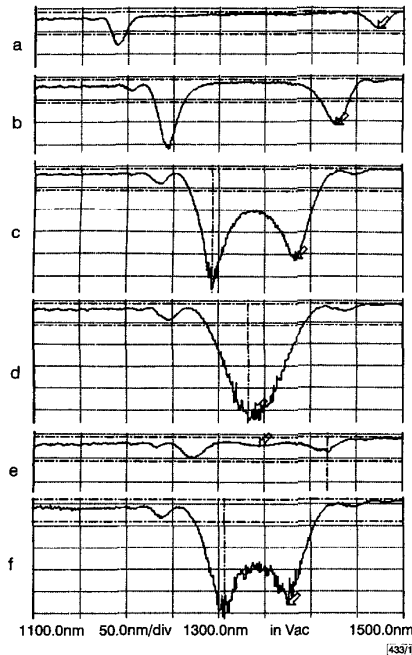


Fig. 1 Transmission spectra of 100 μm period LPG in second exposure and annealing process

a Initial
b After 2000 shots
c After 10000 shots
d After 15000 shots
e After 25000 shots
f After annealing

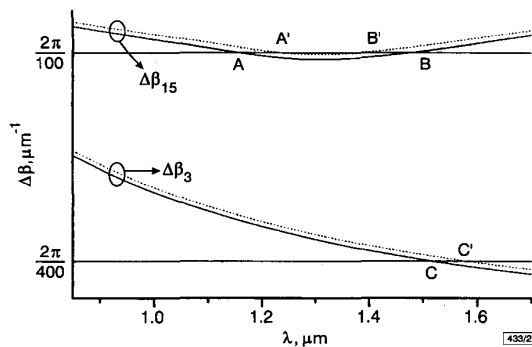


Fig. 2 Graphic method for analysis of shifts of resonant peaks of LPGs

— initial
..... exposed

Discussion: To analyse the shifts in the resonant peaks of the LPGs, we used a graphic method. Curves for $\Delta\beta_m$, the difference in propagation constant between the LP_{01} core mode and LP_{0m} cladding mode, are plotted against wavelength in Fig. 2. The propagation constants of the core and cladding modes of the fibre used in our experiment result from the numerical solutions to the dispersion equations [9]. The horizontal lines $2\pi/\Lambda$ in Fig. 2 represent the gratings with given periods of Λ . The intersection points of the $\Delta\beta_m(\lambda)$ curves and the horizontal lines are the wavelengths at which the phase matching conditions are satisfied. Calculation shows that the $\Delta\beta_{15}(\lambda)$ curve is the only one that intersects the hor-

izontal line $2\pi/100$ at wavelengths ranging between 1100 and 1500 nm. For clarity, other curves are not plotted in Fig. 2, while the $\Delta\beta_3(\lambda)$ curve is plotted for comparison. The intersection points A and B for the initial grating, as shown in Fig. 2, indicate that the LP_{015} cladding mode has two resonant wavelengths in the 100 μm period grating. Therefore, it is considered that the two resonant peaks in Fig. 1*a* both result from the coupling to the LP_{015} cladding mode. When the average core index increases, the $\Delta\beta_m(\lambda)$ curves will move upwards, as shown by the dotted curves in Fig. 2, and the points A and B shift to A' and B', respectively. It is evident that A' and B' can move closer and even disappear as long as the average core index is large enough. Because exposure increases the average core index while annealing decreases it, all the observed shifts in resonant wavelengths in Fig. 1 can be well explained by the graphic method. If the two peaks in Fig. 1 are assumed to result from different order cladding modes, they could not coincide with each other because the $\Delta\beta_m(\lambda)$ curves never intersect each other. So we conclude that they belong to the same cladding mode. As for the LP_{03} mode in a 400 μm period grating shown in Fig. 2, only one resonant peak is observed, which shifts towards longer wavelengths as the average core index increases. Comparing the $\Delta\beta_{15}(\lambda)$ curve with $\Delta\beta_3(\lambda)$ curve in Fig. 2, it is found that their slopes are quite different. Therefore, physical insight into the seemingly peculiar behaviour of higher order cladding modes in LPGs can be gained as follows: the slopes of the $\Delta\beta_m(\lambda)$ curves for higher order cladding modes turn from negative to positive, while those for lower order modes are always negative.

The reason for the increased depths of the resonant peaks when exposed without the amplitude mask is still under discussion. We assume that the increased index modulation might be associated with the inhomogeneous distribution of Ge-related defects that formed in the first exposure process.

The temperature sensitivity of the two resonant peaks of the initial grating is measured to be 15.5 and $-10.1 \text{ nm}/100^\circ\text{C}$, respectively. If this separation is to be used in sensing, the measured sensitivity for temperature will be greatly improved.

Although we have shifted the peaks over a large range, a smaller tuning range can easily be achieved by carefully controlling the shots. In other experiments, we have tuned the peaks of 400 μm period LPGs from 2 to 20 nm.

Conclusions: We have demonstrated that coupling between the guided fundamental core mode and a higher order cladding mode may lead to dual resonant peaks. The observation of the shifts of both peaks was achieved using a 100 μm period LPG. A theoretical explanation has been made through the use of a simple graphic method. This information provides additional insight into the characteristics of the resonant wavelengths of LPGs. It has also been demonstrated that the resonant wavelengths of LPGs can be tuned over a large wavelength range by the post-exposure technique, which potentially provides the fabrication of LPGs with flexibility.

Acknowledgment: The authors would like to thank Xiaoyi Da, Haojun Fu and Jianguo Yu for helpful discussions and encouragement. The work is supported by the National Natural Science Foundation of China.

© IEE 1999

Electronics Letters Online No: 19990442
DOI: 10.1049/el:19990442

12 February 1999

Xuwen Shu, Zhijian Huang and Dexiu Huang (Department of Optoelectronics, Huazhong University of Science and Technology, Wuhan, Hubei, 430074, People's Republic of China)

Xuemei Zhu, Qinglin Wang, Shan Jiang and Wei Shi (Solid Device Research Institute, Wuhan Research Institute of Posts and Telecommunications, Wuhan, Hubei, 430074, People's Republic of China)

References

- VENGSAKAR, A.M., LEMAIRE, P.J., JUDKINS, J.B., BHATIA, V., ERDOGAN, T., and SIPE, J.E.: 'Long-period fiber gratings as band-rejection filters', *J. Lightwave Technol.*, 1996, **14**, (1), pp. 58-65
- VENGSAKAR, A.M., LEMAIRE, P.J., JACOBOWITZ-VESELKA, G., BHATIA, V., and JUDKINS, J.B.: 'Long-period fiber gratings as gain-flattening and laser stabilizing devices'. Proc. IOOC'95, Hong Kong, June 1995, Postdeadline Paper PD1-2

- 3 LEE, B.M., and NISHII, J.: 'Notch filters based on cascaded multiple long-period fibre gratings', *Electron. Lett.*, 1998, **34**, (19), pp. 1872-1873
- 4 HILL, K.O., MALO, B., VINEBERG, K., BILODEAU, F., JOHNSON, D., and SKINNER, I.: 'Efficient mode conversion in telecommunication fibre using externally written gratings', *Electron. Lett.*, 1990, **26**, (16), pp. 1270-1272
- 5 PATRICK, H.J., CHANG, C.C., and VOHRA, S.T.: 'Long period fibre gratings for structural bend sensing', *Electron. Lett.*, 1998, **34**, (18), pp. 1773-1775
- 6 EDOGAN, T.: 'Cladding-mode resonances in short- and long-period fibre grating filters', *J. Opt. Soc. Am. A*, 1997, **14**, (8), pp. 1760-1773
- 7 PATRICK, H.J., KERSEY, A.D., and BUCHOLTZ, F.: 'Analysis of the response of long period fiber gratings to external index of refraction', *J. Lightwave Technol.*, 1998, **16**, (9), pp. 1606-1612
- 8 MACDOUGALL, T.W., PILEVAR, S., HAGGANS, C.W., and JACKSON, M.A.: 'Generalized expression for the growth of long period gratings', *IEEE Photonics Technol. Lett.*, 1998, **10**, (10), pp. 1449-1451
- 9 MONERIE, M.: 'Propagation in doubly clad single-mode fibers', *IEEE Trans.*, 1982, **MTT-30**, (4), pp. 381-388

Electro-optical upconversion in chirped fibre grating based true time delay lines

J.L. Corral, J. Marti, P. Matthews and P. Biernacki

An investigation is presented into the use of an electro-optical upconverting modulation scheme on chirped fibre grating based true time delay lines, and analyses made of both the amplitude and delay of detected microwave signals. The bandwidth limitation of the delay line due to the fibre grating dispersion is clearly improved over that in conventional modulation schemes, while the time delay performance is kept constant ($\sigma_{max} = \pm 0.9$ ps).

Introduction: Recently, there has been strong interest in employing chirped fibre gratings (CFGs) as continuously variable true time delay elements in optical beamforming networks for microwave and millimetre-wave phased array antennas [1, 2]. CFGs have been demonstrated to perform well in the realisation of true time delay lines, but some limitations on the available bandwidth due to the CFG dispersion have been reported [3]. Dual-drive optical modulators operating as single sideband plus carrier (SSB+C) generators have been proposed to overcome the dispersive attenuation on the detected signal [3]. Conversely, electro-optical harmonic upconverting schemes are being considered in millimetre-wave antenna systems in order to reduce the requirements on the bandwidth of lasers or external modulators. The optical upconversion of an intermediate frequency (IF) signal, which directly modulates a narrowband laser, through a Mach-Zehnder electro-optical modulator (MZM) driven by a local oscillator (LO) signal which is biased at its minimum transmission bias (MTB) point, has been recently demonstrated which could lead to a significant reduction in chromatic dispersion effects in standard fibre optic links [4]. In this Letter, the use of this MTB up-converting scheme on CFG based true time delay lines is proposed and demonstrated. The results show that the bandwidth limitation due to the CFG dispersion is mitigated, while true time delay performance and optical carrier wavelength dependence are maintained.

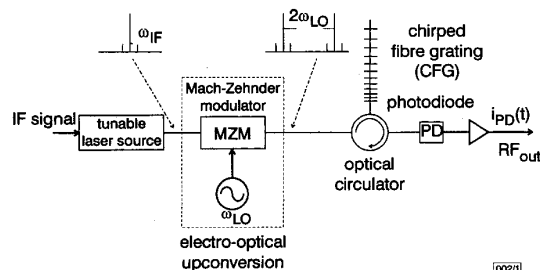


Fig. 1 CFG time delay unit with pseudo-self-heterodyne modulation scheme

Analysis: The proposed configuration for a continuously variable true time delay line with good performance for millimetre-wave frequencies employing a pseudo-self-heterodyne (PSH) technique is shown in Fig. 1. An optical signal intensity-modulated (either directly or externally) with an IF electrical signal is up-converted through an MZM driven by a local oscillator signal (with angular frequency ω_{LO}) and biased at the MTB point. After the MZM, the optical signal is basically composed of two optical carriers separated by $\Delta\omega = 2\omega_{LO}$ and both modulated by the intermediate frequency. As both carriers are IF modulated, not a true self-heterodyne, but a PSH modulation scheme is achieved. Finally, the optical signal passes through a linear CFG, which introduces a time delay that may be varied by tuning the optical wavelength of the laser. The CFG group delay behaviour is characterised by its group delay slope δ (ps/nm). Assuming that the upconverting MZM is driven by a low level signal, second-order terms are negligible and the component of the detected signal at $f_{RF} = 2f_{LO} + f_{IF}$ may be expressed as

$$i_{pd-sel}(f_{RF}) \propto m_{IF} J_1^2(m_{LO}/2) \cos(\lambda_0^2 \pi \delta f_{RF} f_{IF} / c) \times \cos(\omega_{RF}(t + \tau) + \phi) \quad (1)$$

where m_{IF} and m_{LO} are the optical modulation indexes of the IF modulation and the upconverting process, λ_0 is the optical wavelength and c is the speed of light in a vacuum. In a true self-heterodyne technique, the CFG dispersion will be translated to the RF domain without any dispersive attenuation, but as both carriers are modulated in the PSH technique, two beat products at $f_{RF} = 2f_{LO} + f_{IF}$ with opposing dispersion terms, are combined after detection, which will lead to a dispersion-free detected signal with a dispersion dependent amplitude as shown in eqn. 1. The time delay, τ , in eqn. 1 could be varied by tuning the laser wavelength according to

$$\tau = \tau_0 + \delta \Delta\lambda \quad (2)$$

where τ_0 is the system group delay at a fixed wavelength and $\Delta\lambda$ is the variation from this reference wavelength.

For comparison, the dispersive attenuation in the detected signal obtained with conventional intensity modulation depends on detected frequency as [2]

$$i_{pd-im}(f_{RF}) \propto m_o \cos(\lambda_0^2 \pi \delta f_{RF}^2 / c) \cos(\omega_{RF}(t + \tau) + \phi) \quad (3)$$

so the detected RF power degradation will depend on the factor $f_{RF} f_{IF}$, instead of f_{RF}^2 , which will improve the available bandwidth of the true time delay unit. For instance, a CFG-based true time delay unit with a group delay slope of $\delta = 800$ ps/nm and a data signal bandwidth of $f_{IF} = 1$ GHz, will show a -3dB bandwidth of 6.4GHz with conventional intensity modulation but 39GHz with the PSH technique.

Experiment and results: The CFG-based true time delay line with PSH modulation depicted in Fig. 1 has been measured for three different values of intermediate frequency ($f_{IF} = 250$ MHz, 500MHz, 1GHz). The CFG used is a 40cm long apodised linearly chirped fibre grating with an average group delay slope, δ , of nearly 850ps/nm from 1547 to 1551nm. The modulation indexes for both the IF modulation and up-conversion processes were nearly $m_{IF} = 0.1$ and $m_{LO} = 0.6$. The local oscillator frequency was varied in 1GHz steps from 1 to 9GHz. Both PSH and conventional modulation schemes have been considered and the calibrated results are shown in Fig. 2. The dispersive attenuation shown in the conventional case (double sideband plus carrier) is fully overcome when using the PSH technique, as expected from eqn. 1. From Fig. 2 it may be observed that the PSH measurements show an almost constant slope growth over the slightly decay from the simulations. This behaviour is due to the laser chirp index which was not considered in eqn. 1. To verify the time delay behaviour described in eqn. 2, i.e. a constant group delay for all frequencies and a linear dependency on the laser wavelength, the phase of the detected signal component at $f_{RF} = 2f_{LO} + f_{IF}$ has been estimated as a function of the detected frequency. In these simulations, actual measurements (amplitude and delay) of the 40cm CFG are included but an ideal performance has been assumed for the remaining elements depicted in the setup shown in Fig. 1. Therefore, the CFG time delay behaviour with PSH modulation is fully and independently evaluated. In Fig. 3, the detected